Astigmatic Blur in Partial Visual Field Exposure Induces Astigmatism Compensation in Developing Chick Eyes

Patience Ansomah Ayerakwah,[1] Byung Soo Kang,[1] Yuanyuan Liang,[1] Henry Ho-Lung Chan,[1–3] Chea-Su Kee,[1–3] and Tsz Wing Leung[1–3]

[1]School of Optometry, The Hong Kong Polytechnic University, Hong Kong, China
[2]Centre for Eye and Vision Research, Hong Kong, China
[3]Research Centre for SHARP Vision, The Hong Kong Polytechnic University, Hong Kong, China

Correspondence: Tsz Wing Leung, School of Optometry, The Hong Kong Polytechnic University, 11 Yuk Choi Rd., Hung Hom, Kowloon, Hong Kong 999077, China; jeffrey.tw.leung@polyu.edu.hk.

Received: March 24, 2025
Accepted: October 6, 2025
Published: October 27, 2025

Citation: Ayerakwah PA, Kang BS, Liang Y, Chan HHL, Kee CS, Leung TW. Astigmatic blur in partial visual field exposure induces astigmatism compensation in developing chick eyes. *Invest Ophthalmol Vis Sci.* 2025;66(13):43. https://doi.org/10.1167/iovs.66.13.43

Purpose. To determine whether localized retinal exposure to astigmatic blur is sufficient to drive compensatory changes in refractive and corneal astigmatism in developing chick eyes.

Methods. One hundred and thirty-six chicks were randomly assigned to nine groups combining three visual field conditions (full, horizontal, or vertical) and three lens treatments: with-the-rule (WTR) astigmatism (+2.00/−4.00 × 90), against-the-rule (ATR) astigmatism (+2.00/−4.00 × 180), or control (plano lens). Objective refraction and A-scan ultrasonography were measured at baseline (post-hatch day 5) and after 7 days of lens treatment, at which time corneal topography was also assessed. Data were analyzed using interocular differences (treated right eye minus untreated left eye) with two-way ANOVA.

Results. Exposure to astigmatic blur induced significant compensatory changes in both refractive and corneal astigmatism, regardless of visual field extent. WTR blur elicited greater compensatory astigmatism than ATR blur (mean difference = 1.20 ± 0.16 DC, $P < 0.001$), with both conditions showing significant compensation compared to controls ($P < 0.001$). Visual field condition had no significant effect on astigmatic compensation ($P \geq 0.19$). In contrast, spherical ametropia development was influenced by visual field exposure, with partial-field conditions inducing mild myopic shifts and deeper anterior chambers compared to full-field exposure ($P < 0.001$).

Conclusions. Localized retinal exposure to astigmatic blur is sufficient to drive compensatory changes in both refractive and corneal astigmatism, indicating that local retinal mechanisms can independently guide astigmatism compensation. In contrast, spherical refractive development appears to be modulated by the extent of visual field exposure.

Keywords: astigmatism, visual field, compensatory, developing, chicks

Refractive astigmatism, characterized by unequal refractive power between the two principal meridians of the eye perpendicular to each other, results in blurred or distorted vision,[1] which includes corneal and internal astigmatism, with the latter being predominantly from the crystalline lens.[2] This optical imperfection is not only common, affecting 27.2% to 42.7% of school-age children in Asian Chinese (≥0.75 diopter cylinder [DC]) and Native American (≥0.50 DC) populations,[3,4] but also clinically significant due to its potential impacts on vision development[2] and quality of life.[5] Although genetic predispositions contribute to the development of astigmatism[6–8] and the biomechanical force from the eyelids has been proposed to influence corneal astigmatism,[9,10] emerging evidence indicates that visual experience, such as digital device use[11,12] and pandemic-related lifestyle shifts,[13,14] also play a crucial role.

Animal studies have further demonstrated that early exposure to astigmatic blur can induce refractive and corneal astigmatism, suggesting an adaptive emmetropization process that modulates eye growth to reduce astigmatic errors.[15,16] In particular, eyes develop an opposing refractive error to partially compensate for imposed blur; for example, they develop against-the-rule (ATR) refractive astigmatism (with a negative cylindrical axis close to 90°) in response to with-the-rule (WTR) astigmatic blur (with a negative cylindrical axis close to 180°), and vice versa.[15–17] This compensatory response involves a change in the optics of the eye, with studies confirming that the cornea partially contributes to the resulting refractive astigmatism by changing its shape.[15] However, as these findings have largely come from experiments using full-field visual stimulation,[15–18] a key question remains: Is full-field retinal stimulation necessary for this compensation, or can spatially localized defocus alone achieve the same effect?

Although the findings of previously published studies have established the importance of visual signals on astigmatism development, the specific mechanisms driving this compensation still require further investigation, with

emerging evidence pointing to the retina as a key modulator. For example, the experimental disruption of retinal circuitry by excitotoxins in chicks has been shown to inhibit compensatory astigmatic development.[16] Furthermore, early exposure to imposed astigmatic blur has been associated with alterations in retinal electrophysiology—specifically, longer implicit times in inner retinal responses compared to controls.[18,19] Although these findings highlight the role of the retina in astigmatism development, the spatial characteristics of the retinal mechanism involved remain unclear. A key factor deserving further consideration is the non-uniform distribution of retinal cells. In chicks, retinal ganglion cells (RGCs) are unevenly distributed,[20–23] with the nasal and temporal regions exhibiting lower density and larger cell sizes compared to other retinal areas.[20,23,24] This regional heterogeneity could have significant implications for how different parts of the retina process astigmatic blur and may ultimately contribute to the development of astigmatism.

This study aimed to determine whether partial visual field exposure to astigmatic blur can induce compensatory astigmatic changes in the developing eye. To address this question, a chick model was employed to compare the effects of full-field exposure to astigmatic blur with those of localized (vertical or horizontal) exposure to astigmatic blur on refractive and corneal astigmatism. Specifically, it was hypothesized that

1. Partial field exposure is sufficient to trigger compensatory responses, indicating that localized retinal mechanisms can independently drive astigmatic compensation.
2. The magnitude of the compensatory response differs between vertical and horizontal exposure, reflecting underlying variations in RGC density and distribution as well as retinal neural networking.

By clarifying the role of localized retinal input in astigmatism development, this research not only advances the understanding of the adaptability of the visual system but also provides insight into the optimization of clinical interventions for refractive correction, including orthokeratology, peripheral defocus-incorporated lenses, and progressive lenses, which introduce varying amounts of astigmatic defocus over the visual field.[2,25–28]

Methods

Animals Husbandry

One hundred and thirty-six White Leghorn chicks (*Gallus gallus domesticus*) were obtained from the Centralized Animal Facility at The Hong Kong Polytechnic University. The chicks were housed in a temperature-controlled environment maintained between 23.0°C and 24.5°C, with an illuminance (white light) of 150 lux at eye level. A 12:12-hour light:dark cycle (lights on at 07:00 AM and off at 7:00 PM) was implemented to regulate circadian rhythms. Food and water were provided ad libitum throughout the study. All procedures adhered to the ARVO Statement for the Use of Animals in Ophthalmic and Vision Research and were approved by the Animal Subjects Ethics Sub-committee of The Hong Kong Polytechnic University (approval number: 21-22/206).

Visual Manipulation

Baseline measurements, including objective refraction and A-scan ultrasonography, were performed on both eyes at post-hatch day 5 (P5). Immediately following these baseline assessments, chicks were randomly assigned to one of nine experimental groups and subsequently underwent visual manipulation (Fig. 1). To induce astigmatism, a bitoric lens (7.6/6.70-mm base curve, 10.8-mm diameter; X-Cel Specialty Contacts, Duluth, GA, USA) with a +2.00 diopter sphere (DS)/−4.00 DC and a spherical equivalent of 0 D was fitted to the right eye. The lens axis was oriented at either 90° or 180° to simulate WTR and ATR astigmatism, respectively. These orientations were chosen because WTR and ATR are the most prevalent forms of refractive astigmatism in human infants and children.[29–31] In the control group, a plano lens (7.50/7.50-mm base curve, 10.8-mm diameter; X-Cel Specialty Contacts) was fitted to the right eye under the same partial field conditions. The control animals in the full-field group were left untreated to serve as a negative control, establishing a baseline for natural refractive development without any visual manipulation (i.e., no lens wear or visual field restriction). The left eye remained untreated in all groups.

We attached a Velcro ring to the periorbital feathers of the treated eye, and the lens was attached to this ring.[15] The astigmatic axis was aligned by referring to the chick's palpebral fissure and horizontal canthus, and alignment marks on the Velcro ring ensured proper orientation after daily cleaning. Lenses were removed briefly (for less than 1 minute) for cleaning once daily using a cotton swab and air blower to maintain clarity.

Visual field conditions were controlled using an opaque paint (PYLOX aerosol paint; Nippon Paint, Hong Kong, China) to restrict visual exposure and allow selective stimulation of specific retinal regions (Fig. 1). To ensure consistency across all experimental groups, a standardized protocol for every lens was employed. Each lens was first marked into four quadrants of approximately 90°. The two opposing quadrants intended to remain clear were then masked for protection, which prevented paint from covering that part of the lens. An opaque black paint was subsequently applied to the unmasked areas. After the paint dried, the protective masking was removed, resulting in a lens with two clear, opposing quadrants and two occluded quadrants.

Chicks in all groups were exposed to one of three visual field conditions: full-field (FF), horizontal-field (HF), or vertical-field (VF). For the partial-field conditions, an opaque black paint with a light transmittance of <0.01% (250–800 nm, measured using a Lambda 650S spectrophotometer; PerkinElmer, Waltham, MA, USA) and a thickness of about 0.05 mm (measured using a J-45 Dial Thickness Gauge; Hans Schmidt & Co., Waldkraiburg, Germany) was applied to restrict vision outside the designated area. Following the 7-day treatment period (P5–P12), objective refraction and A-scan ultrasonography were repeated. Corneal topography was evaluated at P12. Baseline corneal topography measurements (P5) were not obtained because the small corneal size limited measurement accuracy at that age.

Measurement Procedures

Objective refraction and A-scan ultrasonography measurements were performed between 08:00 AM and 11:00 AM

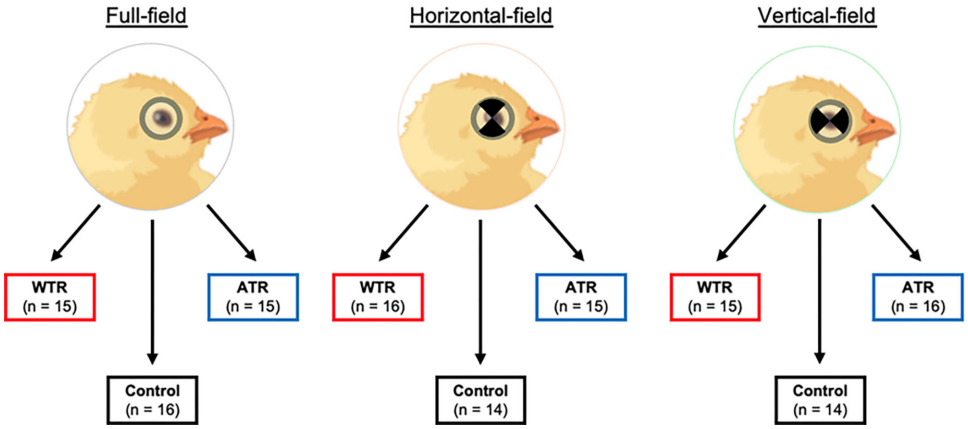

Figure 1. Experimental groups and visual field conditions. Chicks were randomly assigned to one of nine experimental groups (n = 136 total). Three visual field conditions were tested: FF (no occlusion), HF (superior and inferior quadrants occluded), and VF (nasal and temporal quadrants occluded). Within each visual field condition, chicks were further divided into three lens treatment groups: WTR astigmatism (+2.00/−4.00 DC at 90°, *red boxes*), ATR astigmatism (+2.00/−4.00 DC at 180°, *blue boxes*), or control (plano lens, *black boxes*). The schematic chick illustrations show the appearance of the lens on the right eye, where *black regions* indicate occluded areas of the visual field. Sample sizes (n) for each group are indicated in parentheses.

to minimize potential diurnal variations.[32] The instruments and protocols used in this study have been previously described.[33] To ensure the integrity of the data, a strict measurement sequence was followed. Corneal topography was always performed first on alert chicks. Subsequently, chicks were anesthetized for the objective refraction measurements. A-scan ultrasonography, which required contacting the cornea, was always performed last. A brief summary of each method is provided below.

Objective Refraction. Objective refraction was performed at P5 and P12 using a Hartinger coincidence refractometer (Model 110; Carl Zeiss Meditec, Jena, Germany). Prior to measurement, chicks were anesthetized with low-dose isoflurane inhalation (1%–1.5% in oxygen) to stabilize eye movement and minimize accommodation fluctuations.[34] A lightweight, custom-made lid retractor, aligned with the horizontal plane of the palpebral fissure, was gently inserted to maintain eyelid opening and avoid contacting the cornea throughout the procedure. This methodology is based on previous work that demonstrated that such retractors do not significantly affect astigmatic measurements using the Hartinger coincidence refractometer in chicks.[34]

Initial alignment was achieved by positioning the chick's eye so that the external light-emitting diode (LED) ring of the refractometer was concentric with the pupil center. When alignment had been confirmed, the LEDs were switched off, and the reflected mires of the refractometer were adjusted to determine refractive status. For each eye, at least three consecutive measurements were recorded and averaged. Spherical ametropia and refractive astigmatism (magnitude and axis) were obtained from the spherical and cylindrical powers measured by the Hartinger coincidence refractometer.

A-Scan Ultrasonography. Axial biometry was measured at P5 and P12 using a high-resolution A-scan ultrasonography system (GE Panametrics, Billerica, MA, USA) equipped with a 50-MHz polymer probe and an adjustable pulse receiver (polyvinylidene fluoride [PVDF]; P150-2-R0.50; GE Panametrics). Measurements were taken after the chicks were anesthetized with low-dose isoflurane inhalation (1%–1.5% in oxygen). The probe was aligned along the pupillary axis while the eye was held open by a lid retractor. To minimize irritation and enhance optimal signal quality while acting as a medium for transmission of the ultrasound waves, ultrasound gel (Aquasonic ultrasound gel; Parker Laboratories, Fairfield, NJ, USA) was applied to the probe surface, and a drop of distilled water was applied to the eye surface. For each eye, three consecutive measurements were obtained and averaged. Key ocular biometric parameters, including anterior chamber depth (ACD), lens thickness (LT), vitreous chamber depth (VCD), and choroidal thickness, were determined from the peaks identified in the A-scan waveform. Axial length (AL) was defined as the distance from the anterior corneal surface to the anterior retinal surface.[35]

Corneal Topography. Corneal topography was measured at P12 using a custom-built Placido-ring videokeratography system.[15,18] Measurements were performed on awake chicks without a lid retractor. After aligning the pupil with the center of the Placido rings, an integrated charge-coupled device (CCD) camera continuously captured images reflected from the corneal surface. For each eye, at least three images were selected based on the following criteria to minimize potential confounding factors, such as optical misalignment and corneal accommodation[15,18,36]:

- Sharp focus—All captured Placido rings are in sharp focus.
- Central alignment—The central Placido rings are properly aligned with the pupil center.
- No sign of accommodation—There is no constriction of the Placido rings, indicating that corneal accommodation is absent.

Selected images were analyzed using a custom MATLAB algorithm to extract corneal power data.[15,18] Corneal astigmatism, calculated from a central 2.8-mm-diameter region, was used for subsequent analysis. This specific diameter was chosen because it provides the least instrumental noise as previously validated.[37]

Statistical Analysis

Refractive errors obtained via objective refraction were converted into the spherical equivalent (SE) error and the J0 and J45 astigmatic components using power vector analysis[38]:

$$SE = S + \frac{C}{2}$$

$$J0 = -\frac{C}{2}\cos 2\alpha$$

$$J45 = -\frac{C}{2}\sin 2\alpha$$

where S is the spherical power, C is the cylindrical power, and α represents the astigmatic axis. Similarly, corneal astigmatism was decomposed into its J0 and J45 components based on the cylindrical power and astigmatic axis. To facilitate comparison with previous studies[15,16] both refractive and corneal astigmatism were reported as a positive value.

Data from objective refraction, corneal topography, and A-scan ultrasonography were analyzed using SPSS Statistics 21.0 (IBM, Chicago, IL, USA). Baseline comparisons (at P5) were conducted using one-way ANOVA, which confirmed no significant differences in refractive errors or axial biometry between groups for either eye, $F(8, 92) < 0.93$, all $P > 0.10$. To isolate the effects of visual manipulation on refractive error development and eye growth and to control for inter-individual variation, interocular differences (treated right eye minus the untreated left eye) were calculated from data obtained at the end of the treatment period (P12). To confirm that the visual manipulations did not systemically affect the contralateral (untreated) eyes, a separate two-way ANOVA on the effects of astigmatic blur and visual field was performed on the P12 data from the left eyes. This analysis confirmed that neither astigmatic blur nor visual field had a significant effect on the primary outcomes (refractive and corneal astigmatism) in the contralateral eyes (all $P > 0.05$). Most biometric parameters in the contralateral eyes were also unaffected (all $P > 0.05$). However, significant effects of astigmatic blur were observed for LT, $F(2, 127) = 8.06$, $P < 0.001$, and VCD, $F(2, 127) = 4.68$, $P = 0.01$. Post hoc tests indicated that the untreated eyes of control chicks had thicker LT and shorter VCD than those of chicks in the WTR and ATR groups (all $p \leq 0.01$). Given that no significant transfer of treatment effects were observed in our primary outcomes, all analyses were performed on interocular differences. The complete data for each eye are presented in Supplementary Tables S1 and S2.

Two-way ANOVAs were performed to assess the main effects of astigmatic blur (WTR, ATR, control) and visual field (FF, HF, VF) and their interactions for each dependent variable (refractive astigmatism, corneal astigmatism, SE error, and axial biometry). Additionally, Pearson correlation analyses were conducted to examine relationships between refractive and corneal astigmatism. Holm–Bonferroni corrections were applied to adjust for multiple comparisons. All statistical tests were two tailed, with significance set at an alpha level of 0.05. Data are presented as mean ± SEM.

Results

Effects of Visual Manipulation on Astigmatism Development

Refractive Astigmatic Changes. Exposure to astigmatic blur induced significant refractive astigmatism in the treated birds compared to controls (Fig. 2). Two-way ANOVA revealed a significant main effect of astigmatic blur (WTR, ATR, control) on interocular differences in the magnitude of refractive astigmatism, $F(2, 127) = 114.15$, $P < 0.001$ (effect size: $\eta_p^2 = 0.64$) and its vector components J0, $F(2, 127) = 161.75$, $P < 0.001$ (effect size: $\eta_p^2 = 0.72$) and J45, $F(2, 127) = 5.20$, $P < 0.001$ (effect size: $\eta_p^2 = 0.08$). Post hoc analyses of the main effect of astigmatic blur demonstrated that the WTR group exhibited a significantly greater magnitude of refractive astigmatism than both the ATR group (mean difference = 1.20 ± 0.16 D, $P < 0.001$) and the control group (mean difference = 2.39 ± 0.16 D, $P < 0.001$). In addition, the ATR group showed significantly greater refractive astigmatism than the control group (mean difference = 1.19 ± 0.16 D, $P < 0.001$).

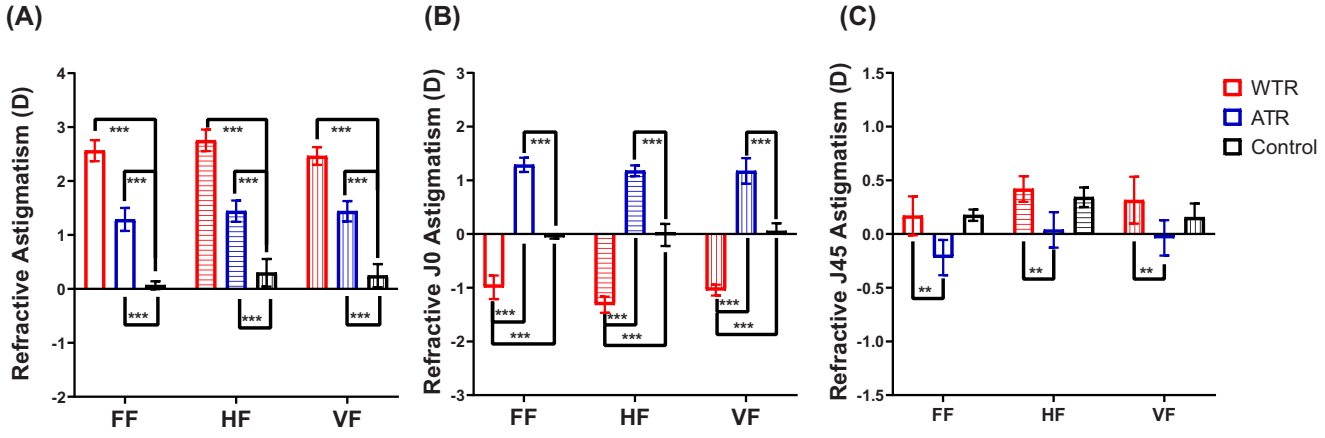

Figure 2. **Refractive astigmatism across different lens treatments and visual field conditions:** (**A**) Magnitude of refractive astigmatism, (**B**) J0 component, and (**C**) J45 component for WTR, ATR, and control groups. Data are presented as interocular differences (treated right eye minus untreated left eye; mean ± SEM). *Red bars* denote WTR groups, *blue bars* denote ATR groups, and *black bars* denote control groups. Within each treatment group, *open bars* indicate FF exposure, *horizontal striped bars* indicate HF exposure, and *vertical striped bars* indicate VF exposure. Significant differences between astigmatic groups are indicated as ***$P < 0.001$.

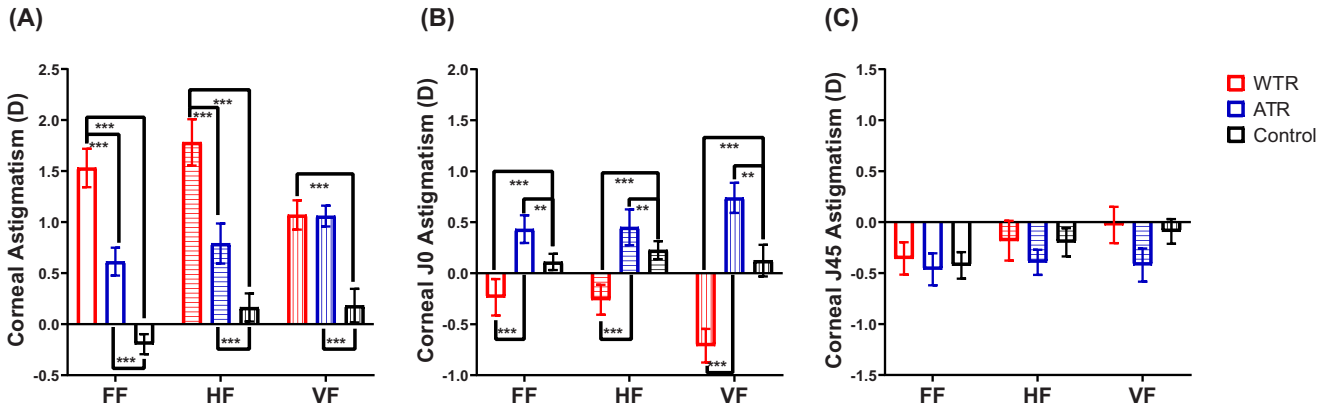

Figure 3. Corneal astigmatism across different lens treatments and visual field conditions: (**A**) Magnitude of corneal astigmatism, (**B**) J0 component, and (**C**) J45 component for WTR, ATR, and control groups. Data are presented as interocular differences (treated right eye minus untreated left eye; mean ± SEM). *Red bars* denote WTR groups, *blue bars* denote ATR groups, and *black bars* denote control groups. Within each treatment group, *open bars* indicate FF exposure, *horizontal striped bars* indicate HF exposure, and *vertical striped bars* indicate VF exposure. Significant differences between astigmatic groups are indicated as ***$P < 0.001$.

Regarding the J0 component, the WTR group developed a more negative value (indicative of ATR astigmatism) than the control group (mean difference = −1.11 ± 0.13 D, $P < 0.001$), whereas the ATR group exhibited a more positive J0 (indicative of WTR astigmatism) than the control group (mean difference = 1.22 ± 0.13 D, $P < 0.001$). The difference between the WTR and ATR groups also reached significance ($P < 0.001$). For the J45 component, the ATR group had a more negative value than both the WTR group (mean difference = −0.37 ± 0.12 D, $P = 0.008$) and the control group (mean difference = −0.30 ± 0.12 D, $P = 0.04$), but no significant difference was found between the WTR and control groups ($P = 0.54$). These findings indicate that induced refractive astigmatism is highly dependent on the axis of the imposed astigmatic blur. In contrast, the visual field condition (FF, HF, VF) showed neither a significant main effect, $F(2, 127) \leq 1.68$, $P \geq 0.19$, nor a significant interaction with astigmatic blur, $F(4, 127) \leq 0.44$, $P \geq 0.78$.

Corneal Astigmatic Changes. Changes in corneal astigmatism were similar to those observed in refractive astigmatism (Fig. 3). Two-way ANOVA revealed a significant main effect of astigmatic blur on both the magnitude, $F(2, 127) = 57.60$, $P < 0.001$ (effect size: $\eta_p^2 = 0.48$), and the J0 component, $F(2, 127) = 10.32$, $P < 0.001$ (effect size: $\eta_p^2 = 0.34$) of corneal astigmatism. Specifically, the WTR group exhibited greater corneal astigmatism than the ATR (mean difference = 0.64 ± 0.13 DC, $P < 0.001$) and control groups (mean difference = 1.41 ± 0.13 DC, $P < 0.001$), but the ATR group also had significantly greater corneal astigmatism than the control group (mean difference = 0.77 ± 0.13 D, $P < 0.001$).

In terms of the J0 component, the WTR group developed a more negative value (indicative of ATR astigmatism) than the control group (mean difference = −0.56 ± 0.12 D, $P < 0.001$), whereas the ATR group exhibited a more positive J0 (indicative of WTR astigmatism) than the control group (mean difference = 0.39 ± 0.12 D, $P = 0.002$). The differences between the WTR and ATR groups were statistically significant ($P < 0.001$).

Although there were no significant main effects of visual field on either the magnitude or the J0 component of corneal astigmatism, $F(2, 127) \leq 2.02$, $P \geq 0.14$, a significant interaction was observed between astigmatic blur and visual field for the magnitude of corneal astigmatism, $F(4, 127) = 3.42$, $P = 0.01$ (effect size: $\eta_p^2 = 0.10$). Within the WTR group, simple main effects analysis revealed that the VF condition induced greater corneal astigmatism than the HF condition (mean difference = 0.71 ± 0.22 D, $P = 0.03$), whereas no significant differences were found between VF and FF ($P = 0.30$) or between HF and FF ($P = 1.00$) conditions. For the J45 component, there were no significant main effects of astigmatic blur, $F(2, 127) = 1.98$, $P = 0.14$, or visual field, $F(2, 127) = 1.79$, $P = 0.17$, nor significant interaction, $F(4, 127) = 0.31$, $P = 0.87$.

Correlations Between Refractive and Corneal Astigmatism. Figure 4 illustrates the relationships between refractive and corneal astigmatism. Pearson correlation analyses revealed that the overall magnitude of refractive astigmatism was moderately to strongly correlated with corneal astigmatism across all visual field conditions (FF, $r = 0.80$; HF, $r = 0.75$; VF, $r = 0.65$; all $P < 0.001$). Similarly, the J0 component of refractive astigmatism was significantly correlated with the J0 component of corneal astigmatism (FF, $r = 0.62$; HF, $r = 0.69$; VF, $r = 0.58$; all $P < 0.001$). In contrast, no significant correlations were observed between the refractive and corneal J45 components after adjusting for multiple comparisons (all $P > 0.05$).

Corneal Curvature Changes. Significant changes in corneal curvature were observed (Fig. 5). For the steepest corneal meridian, a two-way ANOVA revealed a significant main effect of visual field, $F(2, 127) = 5.54$, $P < 0.01$ (effect size: $\eta_p^2 = 0.08$), but no significant main effect of astigmatic blur, $F(2, 127) = 0.23$, $P = 0.80$). There was no significant interaction between these factors, $F(4, 127) = 0.23$, $P = 0.92$. Post hoc analysis of the visual field effect showed that the FF condition resulted in a less steep cornea compared to the VF condition (mean difference = −1.11 ± 0.35 D, $P < 0.01$). No other significant differences between the visual field groups were observed ($P \geq 0.06$).

For the flattest corneal meridian, a two-way ANOVA revealed significant main effects for both astigmatic blur, $F(2, 127) = 8.52$, $P < 0.001$ (effect size: $\eta_p^2 = 0.12$), and visual field, $F(2, 127) = 4.06$, $P = 0.02$ (effect size: $\eta_p^2 = 0.06$). Post hoc tests for the astigmatic blur effect showed

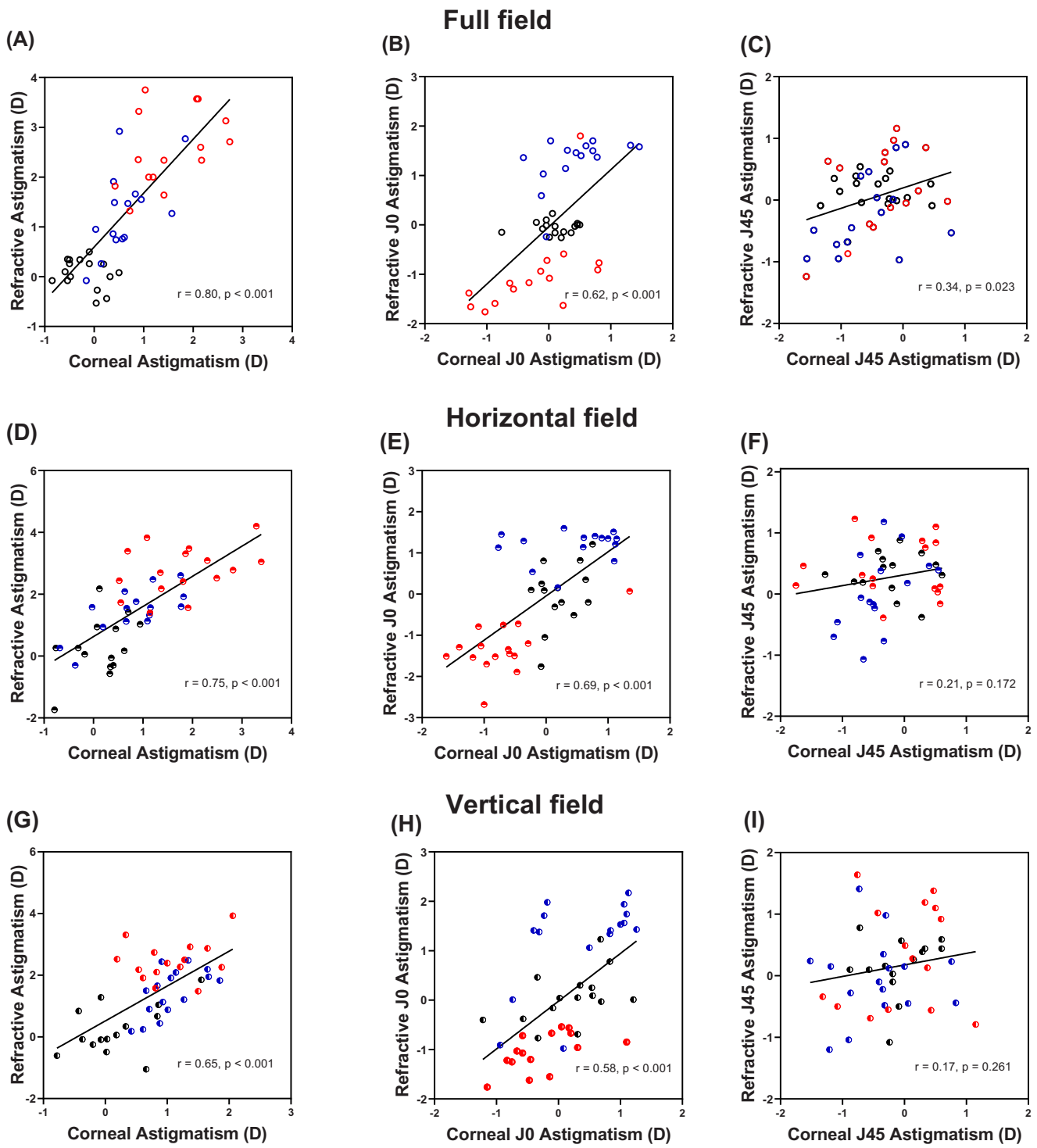

Figure 4. Correlation between corneal and refractive astigmatism. (**A–I**) Scatterplots show the correlation between interocular differences in refractive and corneal astigmatism for the FF (**A–C**), HF (**D–F**), and VF (**G–I**) conditions. The correlations are shown for the magnitude of astigmatism (**A**, **D**, **G**), the J0 component (**B**, **E**, **H**), and the J45 component (**C**, **F**, **I**). Within each panel, *red circles* represent the WTR group, *blue circles* represent the ATR group, and *black circles* represent the control group. Linear regression lines are shown for each visual field condition.

that the WTR group had a significantly flatter cornea than the control group (mean difference = −1.49 ± 0.36 D, $P < 0.001$); other pairwise comparisons were not significant ($P \geq 0.10$). For the visual field effect, post hoc analysis showed that the FF condition had a significantly flatter cornea than the VF condition (mean difference = −1.00 ± 0.36 D, $P = 0.02$); other comparisons were not significant ($P \geq 0.51$).

Investigative Ophthalmology & Visual Science

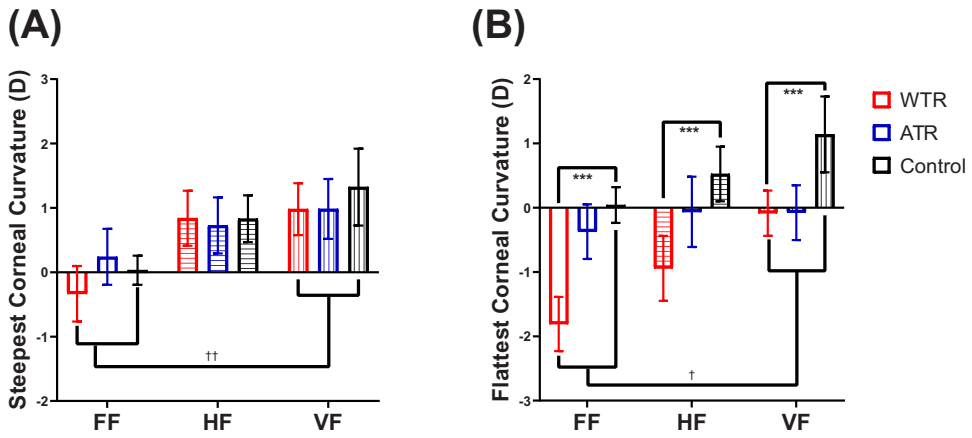

Figure 5. Corneal curvature across different lens treatments and visual field conditions: (**A**, **B**) Magnitude of steepest (**A**) and flattest (**B**) corneal curvatures for WTR, ATR, and control groups. Data are presented as interocular differences (treated right eye minus untreated left eye; mean ± SEM). *Red bars* denote WTR groups, *blue bars* denote ATR groups, and *black bars* denote control groups. Within each treatment group, *open bars* indicate FF exposure, *horizontal striped bars* indicate HF exposure, and *vertical striped bars* indicate VF exposure. Significant differences between refractive groups are indicated as $^{***}P < 0.001$. Significant differences between visual field groups are indicated as $^{\dagger}P < 0.05$, $^{\dagger\dagger}P < 0.01$.

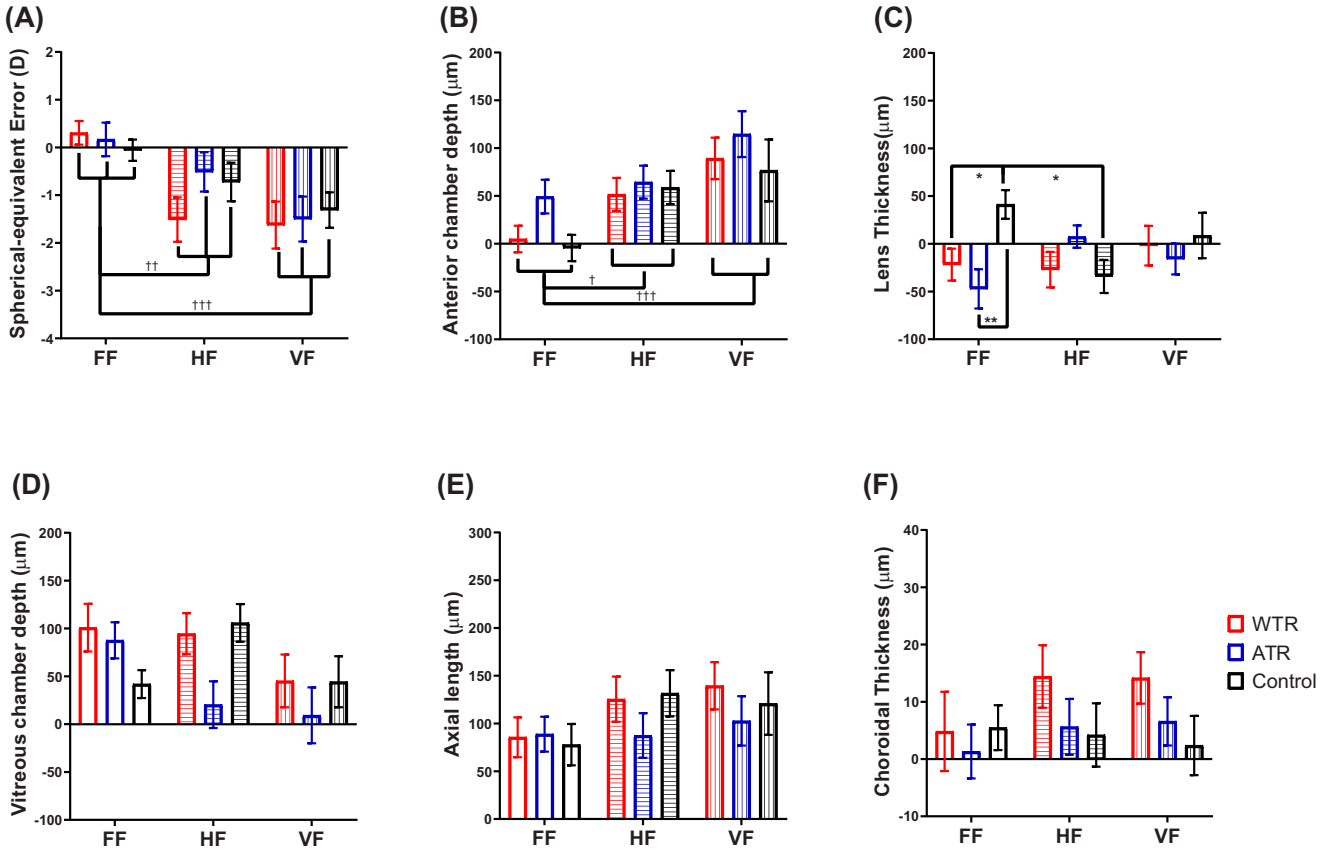

Figure 6. SE error and ocular biometric parameters across different lens treatments and visual field conditions: (**A**) SE error, (**B**) ACD, (**C**) LT, (**D**) VCD, and (**E**) AL for WTR, ATR, and control groups. Data are presented as interocular differences (treated right eye minus untreated left eye; mean ± SEM). *Red bars* denote WTR groups, *blue bars* denote ATR groups, and *black bars* denote control groups. Within each treatment group, *open bars* indicate FF exposure, *horizontal striped bars* indicate HF exposure, and *vertical striped bars* indicate VF exposure. Significant differences between refractive groups are indicated as $^{*}P < 0.05$, $^{**}P < 0.01$. Significant differences between visual field groups are indicated as $^{\dagger}P < 0.05$, $^{\dagger\dagger}P < 0.01$, $^{\dagger\dagger\dagger}P < 0.001$.

Effects of Visual Manipulation on Spherical Ametropia Development and Axial Eye Growth

In contrast to refractive astigmatism, which was significantly influenced by imposed astigmatic blur, changes in spherical ametropia and axial eye growth were primarily driven by visual field conditions (Fig. 6). Astigmatic blur did not significantly affect SE, ACD, LT, VCD, AL, or ChT, $F(2, 127) \leq 2.54$, $P \geq 0.08$. In contrast, visual field conditions had a significant effect on SE, $F(2, 127) = 14.96$, $P < 0.001$ (effect size: $\eta_p^2 = 0.19$); ACD, $F(2, 127) = 8.68$, $P < 0.001$ (effect size: $\eta_p^2 = 0.15$); and VCD, $F(2, 127) = 3.28$, $P = 0.04$ (effect size: $\eta_p^2 = 0.05$). No significant interactions between astigmatic blur and visual field were observed for any of these measures, $F(4, 127) \leq 2.00$, $P \geq 0.10$.

Post hoc analyses revealed that chicks in the FF condition had a significantly more positive SE than those in the VF (mean difference = +1.70 ± 0.32 D, $P < 0.001$) and HF (mean difference = +1.13 ± 0.32 D, $P < 0.001$) conditions. In addition, the FF condition had a significantly shorter ACD than both the VF (mean difference = −72.70 ± 17.52 µm, $P < 0.001$) and HF conditions (mean difference = −41.83 ± 17.52 µm, $P = 0.04$). There were no significant differences in SE or ACD between the VF and HF conditions ($P \geq 0.08$). Although the VF condition tended to yield a shorter VCD than both the HF (mean difference = −42.65 ±13.53 µm, $P = 0.08$) and FF conditions (mean difference = −43.80 ±19.42 µm, $P = 0.08$), these differences did not reach statistical significance. Similarly, the difference in VCD between the FF and HF conditions was not significant ($P = 0.95$).

For LT, neither astigmatic blur nor visual field had significant main effects, $F(2, 127) \leq 1.66$, $P \geq 0.19$. However, a significant interaction was observed between these factors, $F(4, 127) = 3.28$, $P = 0.01$ (effect size: $\eta_p^2 = 0.09$). Simple main effects analysis within the control group revealed that the HF condition resulted in a significantly thinner LT than the FF condition (mean difference = −75.43 ± 25.31 µm, $P = 0.02$), whereas no significant differences were found between VF and HF or VF and FF conditions ($P \geq 0.25$). Within the FF condition, the control group exhibited a significantly thicker LT than either WTR (mean difference = 63.03 ± 24.86 µm, $P = 0.03$) or ATR (mean difference = 88.53 ± 24.86 µm, $P = 0.003$) groups, with no significant difference between the WTR and ATR groups ($P = 0.31$). For AL and ChT, there were no significant main effects of astigmatic blur or visual field, $F(2, 127) \leq 1.90$, $P \geq 0.15$, nor significant interaction, $F(4, 127) \leq 0.51$, $P \geq 0.73$.

Discussion

Two primary findings were observed in this study. First, localized retinal exposure to astigmatic blur was sufficient to induce compensatory changes in both refractive and corneal astigmatism in developing chick eyes, regardless of full or partial visual field conditions. Second, in contrast, changes in SE error and ACD were primarily modulated by the extent of visual field exposure, with partial-field conditions leading to more pronounced myopic shifts compared to FF conditions. This suggests that spherical refractive development, unlike astigmatism compensation, is influenced by the regional distribution of visual input across the retina.

Localized Retinal Mechanisms in Astigmatism Compensation

Our results demonstrate that, even when astigmatic blur is restricted to only a portion of the visual field, the compensatory response remains robust. Thus, the presence of astigmatic blur is essential to drive compensatory response. Notably, partial-field exposure was as effective as FF stimulation in triggering compensatory responses, suggesting that the retina integrates signals over a limited spatial extent. It can be hypothesized that this integration may be mediated by horizontal and wide-field amacrine cells, which are known to facilitate lateral signal transmission in vertebrate retinas,[39] although direct evidence in chicks is still lacking. In addition, diffusible factors such as dopamine,[40,41] which has been implicated in the regulation of eye growth,[42,43] could contribute to the propagation of astigmatic signals across the retina. However, the specific roles of these neural circuits and diffusible factors in mediating astigmatism compensation remain to be fully determined. Future studies should explore whether horizontal and wide-field amacrine cells directly transmit astigmatic growth signals in the chick retina and clarify the contribution of dopamine to astigmatism development.

Despite regional differences in RGC density and distribution in the chick retina,[20,23,24] the orientation and magnitude of both refractive and corneal astigmatism were similar under FF, HF, and VF conditions. These results underscore a remarkable capacity for localized retinal mechanisms to detect and respond to astigmatic blur. The findings are consistent with previous studies that imposed FF astigmatic blur in chicks, in which the magnitude of astigmatism developed differed in response to WTR and ATR conditions.[15,16] Specifically, compensatory astigmatism was strongly dependent on the orientation of the imposed blur: Exposure to WTR astigmatic blur elicited a larger compensatory shift, resulting in astigmatism oriented in the ATR direction. In contrast, exposure to ATR astigmatic blur produced a smaller compensatory shift oriented in the WTR direction, as reflected by changes in the J0 vector component.[15,16,18] The absence of significant astigmatic changes in control groups under all visual field conditions confirms that these compensatory effects are driven by the imposed astigmatic blur rather than by visual field occlusion per se.

Furthermore, the significant correlation between corneal and refractive astigmatism supports the notion that corneal remodeling actively contributes to the compensatory process. Across all visual field conditions, corneal astigmatism accounted for approximately 42% to 64% of the variation in the magnitude of refractive astigmatism and 34% to 45% of the variation in the J0 component. Although these correlations are lower than those typically reported in human studies,[44–46] they align well with previous findings in chick models.[15,34] The analysis of the principal corneal meridians revealed the mechanism for this remodeling: The imposed astigmatic blur selectively altered the flattest meridian without significantly affecting the steepest one. Specifically, in response to WTR blur, the eye flattened the primarily vertical meridian. This remodeling resulted in compensatory ATR corneal astigmatism, with an axis of 102° (calculated from the average J0 and J45 values in Figs. 3B and 3C). Conversely, in response to ATR blur, the eye flattened the primarily horizontal meridian, leading to compensatory WTR astigmatism with an axis of 161°. This asym-

Investigative Ophthalmology & Visual Science

metric change to a single meridian explains the resulting compensatory shift in corneal astigmatism.

Interestingly, the difference in the magnitude of corneal astigmatism induced by WTR and ATR blur was absent in the VF condition (Fig. 3A). Furthermore, VF exposure, regardless of the induced blur, also led to significant anterior segment changes, including a steeper cornea and deeper anterior chamber, compared to FF exposure (Figs. 5, 6B). Although the mechanism linking these observations is not yet understood, our results show a disparity between the corneal and overall refractive responses of the eye. Crucially, despite the altered corneal remodeling pattern observed in the VF group, the final refractive astigmatic compensation remained effective and was comparable across all visual field conditions. This disparity suggests that, when the corneal contribution to compensation is altered, other optical components, most plausibly the crystalline lens, adjust to achieve the necessary refractive outcome. Future studies are warranted to directly measure the properties of the crystalline lens to confirm its compensatory role in response to partial-field astigmatic blur.

Restricted Visual Field Influences Spherical Ametropia Development and Axial Eye Growth

Partial-field conditions induced mild myopic shifts ranging from -0.51 ± 0.41 D to -1.63 ± 0.49 D relative to FF conditions. Importantly, these myopic shifts cannot be attributed to the imposed astigmatic blur. Under FF conditions, both WTR and ATR astigmatism resulted in mild hyperopia ($+0.31 \pm 0.25$ D and $+0.40 \pm 0.28$ D, respectively), values that were not significantly different from those of the control group (-0.06 ± 0.22 D). These observations are consistent with previous studies in chicks and monkeys that have shown that FF astigmatic blur, even when coupled with varying spherical errors, tends to direct refractive development toward the circle of least confusion or toward a more hyperopic focal plane.[15,18,47] In our FF conditions, the use of cross-cylindrical lenses with zero SE error resulted in mild hyperopia near the circle of least confusion. Thus, the myopic shifts observed under partial-field occlusion are most likely attributable to the restricted visual input rather than by the imposed astigmatism.

The mechanisms by which partial-field occlusion influence SE error and axial biometric parameters remain unclear. Notably, the findings of this study differ substantially from those observed in form deprivation myopia (FDM). In FDM, diffusers transmit light while disrupting form vision,[48] which typically leads to substantial axial elongation and high myopia (over -20 D after 1 week).[49] In contrast, the use of opaque black paint blocked nearly all light, resulting in only modest refractive and structural changes, primarily manifesting as anterior chamber deepening. In addition, changes in LT, VCD, and AL were minimal or exhibited interactions with the imposed astigmatic blur. These differences suggest that distinct mechanisms underlie the ocular changes induced by restricted visual input compared to those driving FDM. Further investigations are needed to elucidate how spatially limited visual input affects ocular growth, particularly in terms of anterior chamber development, and to clarify the underlying mechanisms involved, as this will help provide insights into the effects of the anterior chamber on the progression of refractive errors.

Limitations

Although this study demonstrated that localized retinal mechanisms can drive astigmatism compensation, there are several limitations that must be acknowledged. First, the use of opaque black paint for partial-field occlusion unexpectedly induced a mild myopic shift, even in the plano partial-field control group. This unintended effect could require caution in the interpretation of spherical error data. Second, the experimental design did not differentiate between the contributions of the central and peripheral retina; partial-field occlusion stimulated both regions simultaneously. Future studies employing more targeted occlusion techniques (for example, using quadrant-specific or central versus peripheral occlusion) are necessary to clarify the distinct roles each retinal region plays in astigmatic compensation. Third, eye movements of the chicks were not controlled in this study. Given that chicks exhibit significant eye movements (up to 40°), predominantly along the horizontal axis,[50] the precise retinal area stimulated by the astigmatic blur was not constant. However, if these eye movements were a primary confounding factor, a different astigmatic response would be expected between the HF and VF groups. Although any influence of eye movement cannot be completely ruled out, the finding that the compensatory astigmatic response was comparable across all visual field conditions suggests that the observed changes were driven by the presence of localized astigmatic blur, rather than by the pattern of eye movements across the occluded zones. Finally, this study only measured central refraction and on-axis biometry. Consequently, it remains unclear whether the myopic shifts observed in the partial-field conditions were localized to the occluded retinal regions, a phenomenon that has been reported in hemifield form-deprivation studies.[51] Future studies incorporating peripheral refraction and eye shape measurements are warranted to clarify the spatial specificity of these ocular growth responses.

Conclusions

This study demonstrates that localized retinal exposure to astigmatic blur, whether applied to the entire or only a portion of the visual field, is sufficient to drive compensatory changes in both refractive and corneal astigmatism in developing chick eyes. These specific visual field responses underscore the role of local retinal circuits in guiding astigmatism compensation. This finding has significant clinical implications, as common myopia control interventions including multifocal contact lenses, orthokeratology, and peripheral defocus spectacle lenses introduce varying patterns of astigmatic blur across the visual field.[52–55] However, the effects of these interventions on astigmatism development in children are not yet well understood. Therefore, future research is necessary not only to elucidate the underlying cellular and molecular mechanisms but also to determine how these local compensatory processes influence refractive outcomes in a clinical setting, ultimately informing the design of more targeted and effective interventions.

Acknowledgments

The authors thank the use of AI technology (Gemini 1.5), a multimodal model developed by Google DeepMind, in editing Figure 1 in February 2025. We gratefully acknowledge Maureen

Valerie Boost, PhD, for her invaluable assistance in editing this manuscript.

Supported by the Innovation and Technology Commission of the HKSAR Government (ITC InnoHK CEVR Project 1.5) and a research fund (P0045838) from the Research Centre for SHARP Vision.

Disclosure: **P.A. Ayerakwah**, None; **B.S. Kang**, None; **Y. Liang**, None; **H.H.-L. Chan**, None; **C.-S. Kee**, None; **T.W. Leung**, None

References

1. Cox MJ. Astigmatism. In: Dartt DA, ed. *Encyclopedia of the Eye*. Cambridge, MA: Academic Press; 2010:135–145.
2. Read SA, Vincent SJ, Collins MJ. The visual and functional impacts of astigmatism and its clinical management. *Ophthalmic Physiol Opt*. 2014;34(3):267–294.
3. Hashemi H, Fotouhi A, Yekta A, Pakzad R, Ostadimoghaddam H, Khabazkhoob M. Global and regional estimates of prevalence of refractive errors: systematic review and meta-analysis. *J Curr Ophthalmol*. 2018;30(1):3–22.
4. He M, Zeng J, Liu Y, Xu J, Pokharel GP, Ellwein LB. Refractive error and visual impairment in urban children in southern China. *Invest Ophthalmol Vis Sci*. 2004;45(3):793–799.
5. Zhang J, Wu Y, Sharma B, Gupta R, Jawla S, Bullimore MA. Epidemiology and burden of astigmatism: a systematic literature review. *Optom Visi Sci*. 2023;100(3):218–231.
6. Lopes MC, Hysi PG, Verhoeven VJM, et al. Identification of a candidate gene for astigmatism. *Invest Ophthalmol Vis Sci*. 2013;54(2):1260–1267.
7. Román-López TV, García-Vilchis B, Murillo-Lechuga V, et al. Estimating the Genetic Contribution to Astigmatism and Myopia in the Mexican Population. *Twin Res Hum Genet*. 2023;26(4-5):290–298.
8. Hammond CJ, Snieder H, Gilbert CE, Spector TD. Genes and environment in refractive error: the Twin Eye Study. *Invest Ophthalmol Vis Sci*. 2001;42(6):1232–1236.
9. Vincent SJ, Collins MJ, Read SA, Carney LG, Yap MK. Corneal changes following near work in myopic anisometropia. *Ophthalmic Physiol Opt*. 2013;33(1):15–25.
10. Wilson G, Bell C, Chotai S. The effect of lifting the lids on corneal astigmatism. *Am J Optom Physiol Opt*. 1982;59(8):670–674.
11. Huang L, Yang GY, Schmid KL, et al. Screen exposure during early life and the increased risk of astigmatism among preschool children: findings from Longhua Child Cohort Study. *Int J Environ Res Public Health*. 2020;17(7):2216.
12. Yang Z, Lu Z, Shen Y, et al. Prevalence of and factors associated with astigmatism in preschool children in Wuxi City, China. *BMC Ophthalmol*. 2022;22(1):146.
13. Liang Y, Kang BS, Kee CS, Leung TW. Compensatory interactions between corneal and internal astigmatism despite lifestyle changes. *Children (Basel)*. 2024;11(2):154.
14. Wong SC, Kee CS, Leung TW. High prevalence of astigmatism in children after school suspension during the COVID-19 pandemic is associated with axial elongation. *Children*. 2022;9(6):919.
15. Chu CHG, Kee CS. Effects of optically imposed astigmatism on early eye growth in chicks. *PLoS One*. 2015;10(2):e0117729.
16. Popa AV, Kee CS, Stell WK. Retinal control of lens-induced astigmatism in chicks. *Exp Eye Res*. 2020;194:108000.
17. Irving EL, Callender MG, Sivak JG. Inducing ametropias in hatchling chicks by defocus—aperture effects and cylindrical lenses. *Vision Res*. 1995;35(9):1165–1174.
18. Vyas SA, Kee CS. Early astigmatism can alter myopia development in chickens. *Invest Ophthalmol Vis Sci*. 2021;62(2):27.
19. Vyas SA, Lakshmanan Y, Chan HHl, Leung TW, Kee CS. Experimentally induced myopia and myopic astigmatism alter retinal electrophysiology in chickens. *Sci Rep*. 2022;12(1):21180.
20. Naito J, Chen Y. Morphological features of chick retinal ganglion cells. *Anat Sci Int*. 2004;79(4):213–225.
21. Chen Y, Wang Z, Shibata H, Naito J. Quantitative analysis of cells in the ganglion cell layer of the chick retina: developmental changes in cell density and cell size. *Anat Histol Embryol*. 2004;33(3):161–167.
22. Naito J, Chen Y. Morphologic analysis and classification of ganglion cells of the chick retina by intracellular injection of Lucifer Yellow and retrograde labeling with DiI. *J Comp Neurol*. 2004;469(3):360–376.
23. Chen Y, Naito J. Regional specialization of ganglion cell layer of the chick retina. *J Vet Med Sci*. 2000;62(1):53–57.
24. Chen Y, Naito J. A quantitative analysis of cells in the ganglion cell layer of the chick retina. *Brain Behav Evol*. 1999;53(2):75–86.
25. Cunha CM, Correia RJB, Neto AAS. Progressive addition lenses: analysis of the power of induced astigmatism. *Rev Bras Oftalmol*. 2013;72(3):164–167.
26. De Lestrange-Anginieur E, Kee CS. Optical performance of progressive addition lenses (PALs) with astigmatic prescription. *Sci Rep*. 2021;11(1):2984.
27. Berntsen DA, Barr CD, Mutti DO, Zadnik K. Peripheral defocus and myopia progression in myopic children randomly assigned to wear single vision and progressive addition lenses. *Invest Ophthalmol Vis Sci*. 2013;54(8):5761–5770.
28. Queirós A, Lopes-Ferreira D, González-Méijome JM. Astigmatic peripheral defocus with different contact lenses: review and meta-analysis. *Curr Eye Res*. 2016;41(8):1005–1015.
29. Namba H, Sugano A, Murakami T, et al. Age-related changes in astigmatism and potential causes. *Cornea*. 2020;39:S34–S38.
30. Leung TW, Lam AKC, Deng L, Kee CS. Characteristics of astigmatism as a function of age in a Hong Kong clinical population. *Optom Vis Sci*. 2012;89(7):84–92.
31. Gwiazda J, Grice K, Held R, McLellan J, Thorn F. Astigmatism and the development of myopia in children. *Vis Res*. 2000;40(8):1019–1026.
32. Nickla DL, Wildsoet CF, Troilo D. Endogenous rhythms in axial length and choroidal thickness in chicks: Implications for ocular growth regulation. *Invest Ophthalmol Vis Sci*. 2001;42(3):584–588.
33. Chu CH, Deng L, Kee CS. Effects of hemiretinal form deprivation on central refractive development and posterior eye shape in chicks. *Vis Res*. 2012;55:24–31.
34. Kee CS, Deng L. Astigmatism associated with experimentally induced myopia or hyperopia in chickens. *Invest Ophthalmol Vis Sci*. 2008;49(3):858–867.
35. Bhardwaj V, Rajeshbhai GP. Axial length, anterior chamber depth-a study in different age groups and refractive errors. *J Clin Diagn Res*. 2013;7(10):2211–2212.
36. Kang BS, Leung TW, Vyas SA, et al. Synchronous myopia development induced by bilateral form deprivation in chicks. *Exp Eye Res*. 2024;239:109783.
37. Chu CHG, Zhou Y, Zheng Y, Kee CS. Bi-directional corneal accommodation in alert chicks with experimentally-induced astigmatism. *Vis Res*. 2014;98:26–34.
38. Thibos LN, Wheeler W, Horner D. Power vectors: an application of Fourier analysis to the description and statistical analysis of refractive error. *Optom Vis Sci*. 1997;74(6):367–375.

Investigative Ophthalmology & Visual Science

39. Lin B, Masland RH. Populations of wide-field amacrine cells in the mouse retina. *J Comp Neurol*. 2006;499(5):797–809.
40. Witkovsky P. Dopamine and retinal function. *Doc Ophthalmol*. 2004;108(1):17–39.
41. Nickla DL, Totonelly K, Dhillon B. Dopaminergic agonists that result in ocular growth inhibition also elicit transient increases in choroidal thickness in chicks. *Exp Eye Res*. 2010;91(5):715–720.
42. Zhou X, Pardue MT, Iuvone PM, Qu J. Dopamine signaling and myopia development: what are the key challenges. *Prog Retin Eye Res*. 2017;61:60–71.
43. McCarthy CS, Megaw P, Devadas M, Morgan IG. Dopaminergic agents affect the ability of brief periods of normal vision to prevent form-deprivation myopia. *Exp Eye Res*. 2007;84(1):100–107.
44. Elkadim M, Nasef MH, Alagorie AR, Allam WA. Corneal topographic versus manifest refractive astigmatism in patients with keratoconus: a retrospective cross-sectional study. *Clin Ophthalmol*. 2022;16:2033–2039.
45. Heidari Z, Mohammad-Rabie H, Mohammadpour M, et al. Correlation between refractive, corneal and residual astigmatism in refractive surgery candidates. *J Mazandaran Uni Med Sci*. 2014;23(110):37–43.
46. Mohammadpour M, Heidari Z, Khabazkhoob M, Amouzegar A, Hashemi H. Correlation of major components of ocular astigmatism in myopic patients. *Contact Lens Anterior Eye*. 2016;39(1):20–25.
47. Kee CS, Hung LF, Qiao-Grider Y, Roorda A, Smith EL, III. Effects of optically imposed astigmatism on emmetropization in infant monkeys. *Invest Ophthalmol Vis Sci*. 2004;45(6):1647–1659.
48. Gisbert S, Feldkaemper M, Wahl S, Schaeffel F. Interactions of cone abundancies, opsin expression, and environmental lighting with emmetropization in chickens. *Exp Eye Res*. 2020;200:108205.
49. Kang BS, Wang LK, Zheng YP, Guggenheim JA, Stell WK, Kee CS. High myopia induced by form deprivation is associated with altered corneal biomechanical properties in chicks. *PLoS One*. 2018;13(11):e0207189.
50. Schwarz JS, Sridharan D, Knudsen EI. Magnetic tracking of eye position in freely behaving chickens. *Front Syst Neurosci*. 2013;7:91.
51. Smith EL, Huang J, Hung LF, Blasdel TL, Humbird TL, Bockhorst KH. Hemiretinal form deprivation: evidence for local control of eye growth and refractive development in infant monkeys. *Invest Ophthalmol Vis Sci*. 2009;50(11):5057–5069.
52. Tomiyama ES, Berntsen DA, Richdale K. Peripheral refraction with toric orthokeratology and soft toric multifocal contact lenses in myopic astigmatic eyes. *Invest Ophthalmol Vis Sci*. 2022;63(8):10.
53. Sauer Y, Scherff M, Lappe M, Rifai K, Stein N, Wahl S. Self-motion illusions from distorted optic flow in multifocal glasses. *iScience*. 2022;25(1):103567.
54. Xu W, Li X, Zhang J, et al. The peripheral defocus designed spectacle lenses might increase astigmatism in myopic children. *Transl Vis Sci Technol*. 2025;14(3):8.
55. Atchison DA, Charman WN, Jaskulski M. Oblique effects with multisegment spectacle lenses: 2. Ray tracing to determine power corrections. *Ophthalmic Physiol Opt*. 2025;45(3):790–798.

Investigative Ophthalmology & Visual Science